

Late Transition Metal Polymerization Catalysis

*Bernhard Rieger, Lisa Saunders Baugh, Smita Kacker,
Susanne Striegler (Eds.)*

B. Rieger, L. Saunders Baugh, S. Kacker, S. Striegler (Eds.)

Late Transition Metal Polymerization Catalysis

Related Titles from WILEY-VCH

I. Marek (Ed.)

Titanium and Zirconium in Organic Synthesis

2000. 400 pages.

Hardcover. ISBN 3-527-30428-2

B. Cornils, W.A. Herrmann (Eds.)

Applied Homogeneous Catalysis with Organometallic Compounds

A Comprehensive Handbook in Three Volumes

2nd Edition, 2002. 1450 pages.

Hardcover. ISBN 3-527-30434-7

B. Cornils, W. A. Herrmann, R. Schlögl, C.-H. Wong (Eds.)

Catalysis from A to Z

A Concise Encyclopedia

2003. ca. 650 pages.

Hardcover. ISBN 3-527-30373-1

M. Beller, C. Bolm (Eds.)

Transition Metals for Organic Synthesis

Building Blocks and Fine Chemicals

2 Volumes

1998 ca. 1062 pages.

Hardcover. ISBN 3-527-29501-1

Late Transition Metal Polymerization Catalysis

*Bernhard Rieger, Lisa Saunders Baugh, Smita Kacker,
Susanne Striegler (Eds.)*

Editors

Prof. Dr. Bernhard Rieger

Inorganic Chemistry II
University of Ulm
Albert-Einstein-Allee 11
89069 Ulm
Germany

Dr. Lisa Saunders Baugh

ExxonMobil Research & Engineering Company
Route 22 East
Annandale, New Jersey 08801
USA

Dr. Smita Kacker

ExxonMobil Chemical Company
5200 Bayway Drive
Baytown, Tx 77520
USA

Dr. Susanne Striegler

Inorganic Chemistry II
University of Ulm
Albert-Einstein-Allee 11
89069 Ulm
Germany

This book was carefully produced. Nevertheless, editors, authors and publisher do not warrant the information contained therein to be free of errors. Readers are advised to keep in mind that statements, data, illustrations, procedural details or other items may inadvertently be inaccurate.

Library of Congress Card No.: applied for

British Library Cataloguing-in-Publication Data

A catalogue record for this book is available from the British Library.

Bibliographic information published by Die Deutsche Bibliothek

Die Deutsche Bibliothek lists this publication in the Deutsche Nationalbibliografie; detailed bibliographic data is available in the Internet at <<http://dnb.ddb.de>>

© 2003 WILEY-VCH Verlag GmbH & Co. KGaA, Weinheim

All rights reserved (including those of translation in other languages). No part of this book may be reproduced in any form – by photoprinting, microfilm, or any other means – nor transmitted or translated into machine language without written permission from the publishers. Registered names, trademarks, etc. used in this book, even when not specifically marked as such, are not to be considered unprotected by law.

Printed in the Federal Republic of Germany
Printed on acid-free paper

Typesetting K+V Fotosatz GmbH, Beerfelden
Printing betz-druck gmbh, Darmstadt
Bookbinding Litges & Dopf Buchbinderei GmbH, Heppenheim

ISBN 3-527-30435-5

Contents

Preface XI

List of Contributors XII

1	Nickel Polymerization Catalysts with Ylide Steering Ligands	1
	<i>Aleksander Ostoja Starzewski</i>	
1.1	Introduction	1
1.1.1	Ylides and Ylidic Bond Systems	1
1.1.2	Ylide Ligand Properties and Coordination Modes	3
1.2	Ylide Nickel Complexes: Novel Polymerization Catalysts	5
1.2.1	Ylide Nickel Complex Synthesis	6
1.2.2	Spectroscopy	6
1.2.2.1	NiPh(Ph ₂ PCHCPhO)(Me ₃ PCH ₂) 1a	7
1.2.3	X-ray Structure Analysis	8
1.3	Ethylene Polymerization	10
1.3.1	Catalyst Activity	10
1.3.2	Novel Ligand Control of PE Molecular Weight	11
1.3.3	Linear and Branched Macromolecules	13
1.3.3.1	Linear Macromolecules	13
1.3.3.2	Short Chain-Branched Macromolecules	13
1.3.3.3	Long Chain-Branched Macromolecules	14
1.3.4	Styryl-Terminated Oligo-/Polyethylenes	15
1.4	Cycloolefin Polymerization	16
1.5	Butadiene Polymerization	17
1.6	Polar Monomer Polymerization	17
1.7	Acetylene Polymerization	18
1.7.1	Catalyst Activity	18
1.7.2	MATPAC, Novel Highly Polar Matrix Polyacetylenes	18
1.7.3	POLPAC [®] , a Tailor-made Polyacetylene Application	22
1.7.4	MATPAC for NLO Devices	23
1.8	References	24

2	Microstructure Control of Ethene Homopolymers Through Tailored Ni,Pd(II) Catalysts 27
	<i>Jürgen Kukral, Alexandra Abele, Gabi Müller, and Bernhard Rieger</i>
2.1	Introduction 27
2.2	Novel 2,6-Diaryl-Substituted Diimine Catalysts: A Versatile Concept for Tailored Polymer Properties from Simple C ₂ Monomers 31
2.2.1	Ligand and Complex Synthesis 32
2.2.2	Solid State Structures 33
2.2.3	Ethene Polymerization Experiments 37
2.2.3.1	Palladium Monomethyl Complexes 37
2.2.3.2	Nickel Dibromides 37
2.3	Desymmetrized Palladium and Nickel Diimine Catalysts 40
2.3.1	Ligand and Complex Synthesis 40
2.3.2	Polymerization Reactions 41
2.4	Palladium Complexes with Bidentate P∩N-Ligands: Application in Ethene Oligomerization 43
2.4.1	Synthesis and Characterization 44
2.4.2	Ethene Oligomerization Reactions 46
2.5	Application of Sterically Demanding Bis(phosphino) Complexes in Ethene Homopolymerization 47
2.5.1	Synthesis and Complexation of Ethene Bridged Bis(phosphine) Ligands 47
2.5.2	Solid State Structures 49
2.5.3	NMR Studies on the Palladium Dichloro Species 52
2.5.4	Influence of Substitution on Ethene Polymerization Reactions 52
2.6	Conclusion 55
2.7	References 56
3	Highly Active Ethene Polymerization Catalysts with Unusual Imine Ligands 59
	<i>Gerrit A. Luinstra, Joachim Queisser, Benno Bildstein, Hans-Helmut Görtz, Christoph Amort, Michael Malaun, Alexander Krajete, Gerald Werne, Marc O. Kristen, Norbert Huber, and Christoph Gernert</i>
3.1	Introduction 59
3.2	Ligand and Metal Complex Synthesis 62
3.2.1	Diimine Systems 62
3.2.1.1	[N,N] Diimines Containing Peripheral N-Heteroaromatic Substituents 62
3.2.1.2	1,2-Diimine Ligands with N-Hetaryl Substituents 64
3.2.1.3	Nickel Complexes with N-Hetaryl 1,2-Diimine Ligands 65
3.2.1.4	Diimine Nickel and Palladium Complexes with 2,6-Dibromophenyl Groups 67
3.2.2	Diimine Pyridine Systems 71

3.2.2.1	[N,N,N] Bis(imino)pyridine Iron and Cobalt Complexes with Peripheral N-Heteroaromatic Substituents	71
3.2.2.2	N-Halogenoaryl-Containing Tridentate Ligands and their Fe Complexes	75
3.2.3	Salicylimine Systems	75
3.2.3.1	[N,O] Salicylimine Nickel Complexes Containing Peripheral N-Heteroaromatic Substituents	75
3.2.4	Ethanol Imine Ligands and their Nickel Complexes	79
3.3	Polymerization Performance	82
3.3.1	Diimine Ni Complexes with Peripheral N-Heteroaromatic Substituents	83
3.3.2	Diiminepyridine Iron and Cobalt Complexes with Peripheral N-Heteroaromatic Substituents	84
3.3.3	Diimine Palladium and Imine Pyridine Iron Complexes with Halogenophenyl Imine Ligands	87
3.3.4	Salicylimine Ni Complexes	91
3.3.5	Hydroxyimine Ni Complexes	91
3.4	Concluding Remarks	95
3.5	Acknowledgements	95
3.6	References	95
4	Cycloaliphatic Polymers via Late Transition Metal Catalysis	101
	<i>Brian L. Goodall</i>	
4.1	Introduction	101
4.2	The Addition Polymerization of Cyclic Olefins	104
4.2.1	Cyclopropenes and Cyclobutenes	104
4.2.2	Cyclopentene	104
4.2.3	Norbornenes	105
4.2.3.1	Nature and Scope of the Catalyst	107
4.2.3.2	Reaction Injection Molding (RIM) of Norbornenes	108
4.2.3.3	Catalyst Synthesis and Polymerization of Norbornene	109
4.2.3.4	On the Mechanism of Initiation	110
4.2.3.5	Poly(norbornene) Microstructure	112
4.2.3.6	On the Mechanism of Propagation and Chain Transfer	113
4.2.3.7	Isolation and Characterization of Norbornene Oligomers	119
4.2.3.8	Control of Glass Transition Temperature	123
4.2.3.9	Multi-Component Catalyst Systems	125
4.2.3.10	Polymerization of Norbornenes Containing Functional Groups	137
4.2.3.11	Polymer Properties and Applications	139
4.3	The Copolymerization of Norbornenes with Acyclic Monomers	144
4.3.1	Copolymers with <i>α</i> -Olefins	144
4.3.1.1	Nickel Catalysts	145
4.3.1.2	Palladium Catalysts	147
4.4	References	150

5	Well-Defined Transition Metal Catalysts for Metathesis Polymerization	155
	<i>Michael R. Buchmeiser</i>	
5.1	Introduction	155
5.2	Transition Metal Alkylidenes	156
5.2.1	Group IVA and VA Transition Metal-Based Initiators	156
5.2.2	Group VI Transition Metal-Based Initiators	157
5.2.2.1	Chromium-Based Initiators	157
5.2.2.2	Tungsten-Based Initiators	157
5.2.2.3	Molybdenum-Based Initiators	161
5.2.3	Group VIIA Transition Metal-Based Initiators	170
5.2.3.1	Rhenium-Based Initiators	170
5.2.4	Group VIIIA Transition Metal-Based Initiators	170
5.2.4.1	Ruthenium-Based Initiators	170
5.2.4.2	Reactivity of Ruthenium-Based Initiators	171
5.2.4.3	Ligand and Structural Variation in Ruthenium-Based Initiators	174
5.2.5	Osmium-Based Initiators	183
5.3	Outlook	183
5.4	References	183
6	Catalysis in Acyclic Diene Metathesis (ADMET) Polymerization	193
	<i>Stephen E. Lehman Jr. and Kenneth B. Wagener</i>	
6.1	Introduction	193
6.2	The ADMET Reaction	195
6.2.1	ADMET: A Step-Growth Polycondensation	195
6.2.2	Functional Group Tolerance	197
6.2.3	Formation of Cyclics	197
6.2.4	<i>Trans</i> -Metathesis	198
6.2.5	General ADMET Mechanism	199
6.2.6	Regiochemical and Stereochemical Considerations	201
6.2.7	Applications of ADMET	202
6.3	Classical Metathesis Catalysts	203
6.4	Well-Defined Tungsten and Molybdenum Catalysts	204
6.5	Well-Defined Ruthenium Catalysts	207
6.5.1	Early Observations: Ill-Defined Ruthenium-Based Catalysts	207
6.5.2	First-Generation Grubbs Catalysts: RuCl ₂ (PR ₃) ₂ CHR ₁	208
6.5.2.1	Synthesis and Activity	208
6.5.2.2	Use in ADMET	210
6.5.3	Second-Generation Grubbs Catalysts: RuCl ₂ (NHC)(PR ₃)CHR ₁	211
6.5.3.1	Synthesis and Activity	211
6.6	Mechanism of ADMET with Grubbs Catalysts	214
6.6.1	Role of the Phosphine Ligand: RuCl ₂ (PR ₃)(L)CHR ₁	214
6.6.2	Role of the L Ligand: RuCl ₂ (PR ₃)(L)CHR ₁	217
6.6.3	Role of the Carbene: the Special Case of the Methylidene	219
6.6.4	Stereochemical Aspects of ADMET	221
6.6.5	Catalyst Decomposition	223

6.7	Experimental Considerations for ADMET	224
6.7.1	The Ideal Case: Bulk ADMET with High Vacuum	224
6.7.2	The Ideal Case: Bulk ADMET with Carrier Gas	224
6.7.3	ADMET with Volatile Monomers	225
6.7.4	Viscous or Solid Monomers of Polymers	225
6.8	Conclusions and Outlook	226
6.9	References	226
7	Transition Metal-Catalyzed Polymerization in Aqueous Systems	231
	<i>Stefan Mecking and Jérôme P. Claverie</i>	
7.1	Introduction	231
7.1.1	Traditional Free-Radical Polymerization in Aqueous Systems	231
7.1.2	General Aspects of Transition Metal-Catalyzed Polymerization in Aqueous Systems	235
7.2	Catalytic Olefin and Alkyne Polymerization in Aqueous Systems	237
7.2.1	Historical Development	237
7.2.2	Recent Progresses in Catalytic Insertion Polymerization of Olefins	238
7.2.2.1	Alternating Olefin/Carbon Monoxide Copolymerization	239
7.2.2.2	Polymerization of Ethylene and 1-Olefins	243
7.2.2.3	Miscellaneous Insertion Polymerizations	249
7.2.3	Recent Progresses in Ring Opening Metathesis Polymerization	231
7.2.4	Recent Progresses in Catalytic Polymerization of Alkynes	254
7.2.4.1	Introduction	254
7.2.4.2	Catalytic Polymerization of Alkynes in Aqueous Systems	256
7.2.5	Summary	258
7.3	Controlled Free-Radical Polymerization in Aqueous Systems with Metal Complexes	259
7.3.1	General Features of Atom Transfer Radical Polymerization (ATRP)	259
7.3.2	Polymerization of Water-Soluble Monomers by ATRP	261
7.3.3	Polymerization of Water-Insoluble Monomers of ATRP	264
7.4	Polymerization by Suzuki-Coupling in Aqueous Systems	266
7.5	Conclusions and Outlook	268
7.6	References	270
8	Copolymerization of Carbon Monoxide with Alkenes	279
	<i>Giambattista Consiglio</i>	
8.1	Introduction	279
8.2	Copolymerization Catalysts and Mechanism	280
8.3	Structure of the Olefin/Carbon Monoxide Copolymers	283
8.4	Catalyst Precursors for the Copolymerization of Ethene	283
8.5	Copolymerization of 1-Olefins	288
8.5.1	Copolymerization of Styrene (and Homologues)	288
8.5.2	Copolymerization of Propene (and Other Aliphatic Olefins)	294
8.6	Copolymerization of Internal and Cyclic Olefins	297
8.6.1	Cyclopolymerization of α,ω -Dienes	299

8.7	Conclusions	300
8.8	References	301

9 Strategies for Catalytic Polymerization of Polar Monomers 307
Ayusman Sen and Myeongsoon Kang

9.1	Introduction	307
9.2	Results and Discussion	307
9.3	Conclusion	316
9.4	References	316

Subject Index	319
----------------------	-----

Preface

Modern polymerization catalysis, as we know it, was triggered by the development of metallocenes and the concomitant understanding of relationships between ligand structure and polymer properties. The manipulation of these useful relationships has led to a renaissance in the synthesis of polyolefin materials having new stereoregularities and, therefore, precise control of polymer rheology.

In contrast to Group IV-based polymerization catalysts, late transition metal complexes can carry out a number of useful transformations above and beyond the polyinsertion reaction. These include isomerization reactions and the incorporation of polar monomers, which have allowed the synthesis of branched polymer chains from ethylene alone, and of functional polyolefins via direct copolymerization. The rational design of metallocene catalysts allowed, for the first time, a precise correlation between the structure of the single site catalyst and the microstructure of the olefin homo- or copolymer chain. A similar relationship does not yet exist for late transition metal complexes. This goal, however, and the enormous opportunities that may result from new monomer combinations, provide the direction and the vision for future developments.

The present book contains nine chapters focusing on the design of imine and phosphorylide catalyst structures, the preparation of cycloaliphatic materials, polar/nonpolar monomer copolymerizations, organometallic polymerizations in aqueous media, and current frontiers in ROMP and ADMET processes. Exactly forty years after the Nobel Prize for Ziegler and Natta, we give a concise description of the state of the art in these fascinating and rapidly developing fields. The authors present, likewise, viewpoints from the forefront of both academia and industrial research, so that basic science and polymer applications are equally covered.

Acknowledgements

We thank all of the chapter authors, primarily for the excellent contributions, but also for their cooperation and their timeliness regarding manuscript submission. We are also grateful for the excellent assistance of Johanna Voegele (Ulm University) with chapter reviews.

Bernhard Rieger, Lisa Saunders Baugh
Smita Kacker, Susanne Striegler

List of Contributors

ALEXANDRA ABELE

Department for Materials and Catalysis
University of Ulm
D-89069 Ulm
Germany

CHRISTOPH AMORT

Institute of General, Inorganic and
Theoretical Chemistry
University of Innsbruck
A-6020 Innsbruck
Austria

BENNO BILDSTEIN

Institute of General, Inorganic and
Theoretical Chemistry
University of Innsbruck
A-6020 Innsbruck
Austria

MICHAEL R. BUCHMEISER

Institute of Analytical Chemistry and
Radiochemistry
University of Innsbruck
Innrain 52a
A-6020 Innsbruck
Austria
E-mail:
michael.r.buchmeiser@uibk.ac.at
Fax: +43 51 25 07 26 77
Tel.: +43 51 25 07 51 84

JEROME P. CLAVERIE

University of New Hampshire
Durham, NH 03824
USA
E-mail: claverie@unh.edu
Fax: +1 603 862 4892

GIAMBATTISTA CONSIGLIO

Departement Chemie
ETH-Hönggerberg
CH-8093 Zürich
Switzerland
E-mail: consiglio@tech.chem.ethz.ch
Fax: +41 16 32 11 62
Tel.: +41 16 32 35 52

CHRISTOPH GERNERT

Department of Chemistry
University of Konstanz
D-78457 Konstanz
Germany

BRIAN L. GOODALL

Formerly of the B. F. Goodrich
Company
Advanced Technology Group
9921 Brecksville Road
Brecksville, OH 44141
USA

Current address:
Research Laboratories
The Rohm and Haas Company
727 Norristown Road
P.O. Box 904
Spring House, PA 19477
USA

HANS-HELMUT GÖRTZ
BASF Aktiengesellschaft
Polymers Research
D-67056 Ludwigshafen
Germany

NORBERT HUBER
Department of Chemistry
University of Konstanz
D-78457 Konstanz
Germany

MYEONGSOON KANG
Department of Chemistry
The Pennsylvania State University
University Park
Pennsylvania 16802
USA

ALEXANDER KRAJETE
Institute of General, Inorganic and
Theoretical Chemistry
University of Innsbruck
A-6020 Innsbruck
Austria

MARC O. KRISTEN
Basell Polyolefine GmbH
D-67056 Ludwigshafen
Germany

JÜRGEN KUKRAL
Department for Materials and Catalysis
University of Ulm
D-89069 Ulm
Germany

STEPHEN E. LEHMAN JR.
The George and Josephine Butler
Polymer Laboratory
University of Florida
P.O. Box 117200
Gainesville, FL 32611-7200
USA

GERRIT A. LUINSTR
BASF Aktiengesellschaft
Polymers Research
D-67056 Ludwigshafen
Germany
and
Department of Chemistry
University of Konstanz
D-78457 Konstanz
Germany

MICHAEL MALAUN
Institute of General, Inorganic and
Theoretical Chemistry
University of Innsbruck
A-6020 Innsbruck
Austria

STEFAN MECKING
Institut für Makromolekulare Chemie
Albert-Ludwigs-Universität
Hermann-Staudinger-Haus
D-79104 Freiburg
Germany
E-mail:
stefan.mecking@makro.uni-freiburg.de
Fax: +49 76 12 03 63 04
Tel.: +49 76 12 03 63 04

GABI MÜLLER
Department for Materials and Catalysis
University of Ulm
D-89069 Ulm
Germany

ALEKSANDER OSTOJA STARZEWSKI
Bayer AG
Wissenschaftliches Hauptlaboratorium
D-51368 Leverkusen
Germany
E-Mail: aleksander.ostojastarzewski.
ao@bayer-ag.de

JOACHIM QUEISSER
BASF Aktiengesellschaft
Polymers Research
D-67056 Ludwigshafen
Germany

BERNHARD RIEGER
Department for Materials and Catalysis
University of Ulm
Albert-Einstein-Allee 11
D-89069 Ulm
Germany

AYUSMAN SEN
Department of Chemistry
The Pennsylvania State University
University Park
Pennsylvania 16802
USA
E-mail: asen@chem.psu.edu

KENNETH B. WAGENER
The George and Josephine Butler
Polymer Laboratory
University of Florida
P.O. Box 117200
Gainesville, FL 32611-7200
USA
E-Mail: wagener@chem.ufl.edu

GERALD WERNE
Department of Chemistry
University of Konstanz
D-78457 Konstanz
Germany

1

Nickel Polymerization Catalysts with Ylide Steering Ligands

ALEKSANDER OSTOJA STARZEWSKI

Abstract

Ylide ligands in nickel catalysts possess a remarkable steering power. Bis(ylide)-nickel complexes provide nonionic organometallic catalyst architectures, which efficiently suppress chain transfer and termination reactions and instead promote chain growth in ethylene polymerizations. Pronounced ligand effects are observed concerning catalyst activity, molecular weight and branching behavior. The catalyst activities without co-catalysts are remarkable in unpolar and even in highly polar solvents. The polar group tolerance makes these catalysts suitable for a variety of polar monomers. Polyacetylene can now be prepared in a controlled fashion in stabilizing highly polar matrices and, in this way, becomes easily processible and even water soluble – ready for high tech applications.

1.1

Introduction

1.1.1

Ylides and Ylidic Bond Systems

Charge distributions and energy levels of phosphorus ylides can be described as the result of specific donor–acceptor interactions between phosphanes and carbenes, resulting in highly polar dative phosphorus–carbon bonds with varying degrees of π -contribution. Similar orbital interactions are also operative with other donor atoms such as nitrogen, arsenic, sulfur or iodine in complexes with carbenes (i.e. in nitrogen, arsine, sulfur ylides), with nitrenes (i.e. in phosphine-imines, arsine-imines, sulfimines), and with oxygen (i.e. in phosphine-oxides, sulfoxides). As a consequence all of these ylidic bond systems exhibit dramatically lower first ionization potentials than normal π -bonds: trimethylphosphine-methylene 6.8 eV versus ethylene 10.5 eV, trimethylphosphine-imine 8.3 eV versus azomethine 12.4 eV, trimethylphosphine oxide 9.9 eV versus formaldehyde 14.4 eV [1–7].

The extreme bond system of phosphorus–carbon ylides, indicated in Eq. (1), is reflected in outstandingly low first ionization potentials (Tab. 1.1).



Photoelectron spectroscopic data place this class of isolable energy-rich compounds on the very top of an energy scale of ligands that do not have a net charge. The molecular property “IE₁” is a quantitative description for the energetic availability of an outermost valence electron and thus a prominent feature of reactivity.

Within a molecular orbital approximation, the electron is ejected from the highest occupied molecular orbital (HOMO). Molecular orbital calculations at various levels of sophistication describe the highest occupied MOs of most ylides as being strongly localized on the ylidic carbon. Exceptions to this are found for example in cyclopentadienide derivatives, where the orbital of corresponding symmetry is the HOMO-1 (IE₂). In terms of reactivity, the low first ionization potentials of ylides reflect high oxidizability, high proton affinity, and basicity. UV photoelectron spectra in conjunction with detailed molecular orbital calculations for each individual ylide structure have made possible a rationalization of the different substituent and heteroatom effects.

Tab. 1.1 Gas-phase UV-PES vertical ionization potentials IE₁ (eV) of phosphorus and arsenic ylides (n_C⁺) and related phosphines (n_P).^{a)}

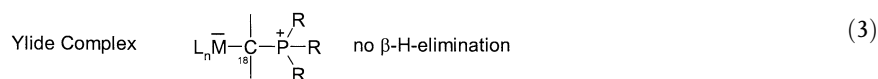
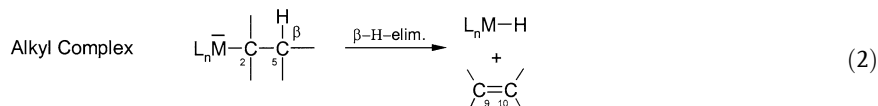
		<i>R</i> = Me	<i>R</i> = Ph
R ₃ PCHCHCHMe	n _C ⁻	6.02	5.95
R ₃ PCHCHCHPh	n _C ⁻	6.20	
R ₃ PCHCHCH ₂	n _C ⁻	6.20	
R ₃ PCHPh	n _C ⁻	6.19	6.01
R ₃ PCHMe	n _C ⁻		6.15
R ₃ PCH ₂	n _C ⁻	6.81	6.62
R ₃ PCHSiMe ₃	n _C ⁻	6.81	6.71
R ₃ PCH(SiMe ₃) ₂	n _C ⁻	6.92	
R ₃ AsCH ₂	n _C ⁻	6.72	
R ₃ AsCHSiMe ₃	n _C ⁻	6.56	
R ₃ AsC(SiMe ₃) ₂	n _C ⁻	6.66	
R ₃ PCp	π _{C=C} /n _C ⁻	6.82/7.02	6.66/6.91
R ₃ PC(CN) ₂	n _C ⁻		7.63
R ₃ P	n _P	8.60	7.80

a) Abbreviations: Me=methyl, Ph=phenyl, Cp=cyclopentadienyl; “n_C” designates ionization from an orbital with largest coefficient on the ylide carbon; “n_P” designates ionization from the phosphorus lone pair orbital.

1.1.2

Ylide Ligand Properties and Coordination Modes

The above-mentioned features of ylides, together with the ability to form ylide anions, and their ease of synthesis make them exciting and versatile ligands for transition metal chemistry [8]. Ylides have outstanding potential with respect to the formation of transition metal–carbon bonds, because a major reaction path for the decomposition of such moieties, i.e. β -H elimination, is blocked by the phosphonium group, a significant difference in comparison with simple alkyl complexes [Eqs. (2) and (3); Fig. 1.1].



Ylides mostly act as σ -carbon ligands with practically no back-bonding characteristics. A variety of ylide–metal structural arrangements have been synthetically accomplished. The organometallic ylide chemistry (Fig. 1.1) covers most of the d-block and some f-block as well as main group elements. It includes mono-, di- and trinuclear

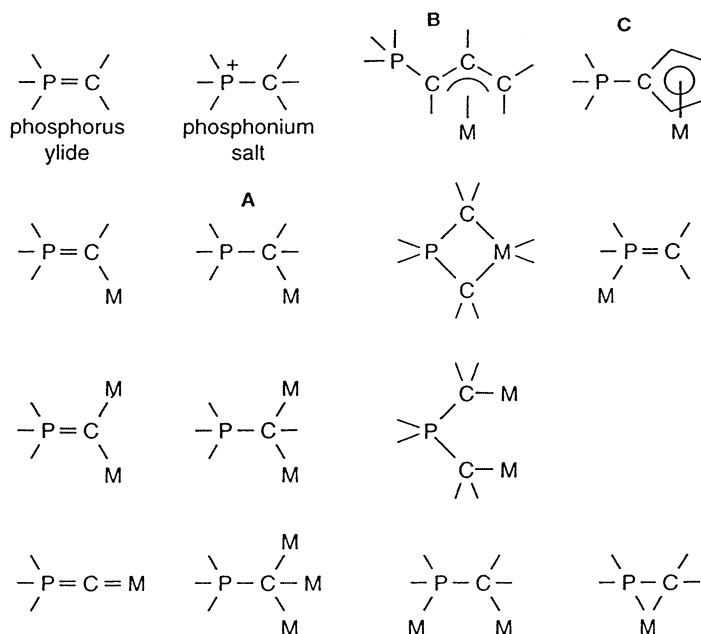


Fig. 1.1 Ylide coordination modes.

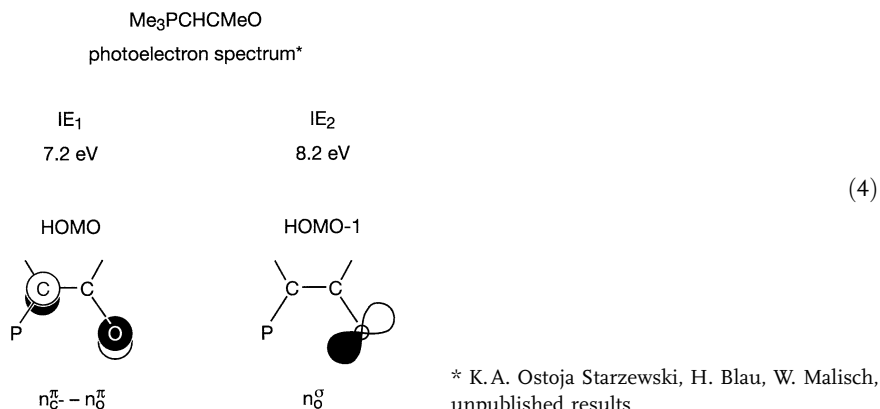
Tab. 1.2 (C=C) π vertical ionization potentials of conjugated ylides IE₂ or IE₁ and related π -hydrocarbons (IE₁).

	IE ₂ or IE ₁ (Ylide) ^{a)} [eV]	IE ₁ (π -Hydrocarbon) [eV]
Me ₃ P=CH-CH=CH ₂	9.02 (IE ₂)	Ethylene: 10.51
Me ₃ P=C ₅ H ₄	6.82 (IE ₁) !	Butadiene: 9.10
Me ₃ P=CH-C ₆ H ₅	8.32 (IE ₂)	Benzene: 9.25

a) Ionization from (C=C) π localized orbitals.

species with ylide ligands sometimes in bridging or in chelating function. In Fig. 1.1, **A** represents the fundamental monodentate σ -complex. Its metal-carbon bond can be described simply as the result of a two electron/two orbital stabilizing interaction between the high lying carbon-centered ylide HOMO “n_C” and a vacant metal orbital. For a given ylide, the degree of complex stabilization depends on the energy of the interacting metal orbital(s), which can be tuned chemically with the other ligands attached to the metal. In **B** and **C** hydrocarbon π -systems are attached to the ylidic carbon which not only results in a delocalization of electron density but also raises the energy levels of the π -substituents with respect to the unperturbed parent π -hydrocarbon, i.e., for the ligands in **B** and **C** relative to ethylene and *cis*-butadiene (Tab. 1.2). In the exceptional case of cyclopentadienyliidene phosphoranes (R₃PC₅H₄) the extreme perturbation of the π -substituent pushes the corresponding *cis*-butadiene level even slightly above that of the ylide bond n_C-level.

The enhanced energetic availability of the substituent π -electrons makes it clear why strongly conjugated ylides may act as polyhapto π -ligands when metal localized orbitals of appropriate symmetry are accessible. In extreme cases the location of highest reactivity may shift into a position remote from the onium center. This “activation” of a substituent, attached to the ylidic carbon, is a general feature and is not limited to CC- π -systems. An impressive example is the photoelectron spectrum of acetylmethylene-trimethylphosphorane, where the low second ionization potential IE₂=8.2 eV originates essentially from an oxygen lone pair orbital [Eqs.



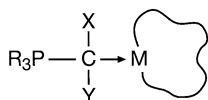
(4) and (5)]. The corresponding lone pair ionization IE_1 of acetaldehyde appears at 10.3 eV, that of formaldehyde at 10.9 eV.



1.2

Ylide Nickel Complexes: Novel Polymerization Catalysts

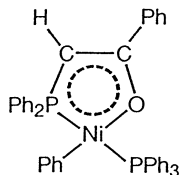
Obviously, ylide complexes such as **1**, in which the ylide ligand is coordinated via the ylidic anion center to a suitable transition metal, are of interest concerning their properties as polymerization catalysts in comparison to commonly used ligands such as phosphanes, which differ significantly in the energetic availability of the ligand lone pair electrons as well as in the ligand donor/acceptor ratio. This chapter reviews research results in this area, obtained in the Central Research Laboratories of Bayer in Leverkusen.



1 phosphorus ylide complex

The organometallic chemistry of nickel has been demonstrated to have outstanding potential in the activation of unsaturated substrates. Nickel-phosphane-based homogeneous catalysts for the CC-linkage of olefins are known to provide synthetic access to dimers, trimers, oligomers and cyclooligomers. Some of these catalysts offer a high degree of control over the stereochemistry of these transformations [9 a, b].

The reaction of the stabilized ylide benzoylmethylene-triphenylphosphorane with Ni(0) in the presence of triphenylphosphane leads to the *oligomerization* catalyst **2**, which catalyzes the reaction of 6000 moles of ethylene per mole of complex at 50 bar and 50 °C. The catalyst **2** is a model system for the “Shell Higher Olefin Process” (SHOP) for the production of liquid *α*-olefins of high linearity, which has been studied in detail by Keim and coworkers at the RWTH Aachen [9c and literature, reviewed in 8].



2 phosphane nickel complex

This system was selected by us to serve as a benchmark for developing new ligand fields, based on the concept of highly polar ylidic bond systems, with the intention of turning low-valent nickel complexes into novel catalysts for *polymerization* instead of for oligomerisation, without the need for co-catalysts. It was hoped that such systems would provide a much broader ligand-based steering potential for optimizing activity, controlling selectivity and for providing catalytic access to new polymeric materials.

1.2.1

Ylide Nickel Complex Synthesis

Our first approach was to react a nickel(0) compound with *two* ylides, one of which was CO-stabilized [Eq. (6)].



We found that the reaction of bis(cyclooctadiene)nickel(0) with the two ylides benzoylmethylene-triphenylphosphorane and methylene-trimethylphosphorane in toluene yields a highly active homogeneous catalyst (**1a**) without any co-catalyst – the ethylene turnover being approximately *tenfold* compared to **2** [10].

Complex formation takes place immediately when the methylene-trimethylphosphorane is added. A yellow solid can be crystallized from the reaction solution in high yield, microanalysis of which shows a Ni/ylide A/ylide B complex with 1/1/1 stoichiometry.

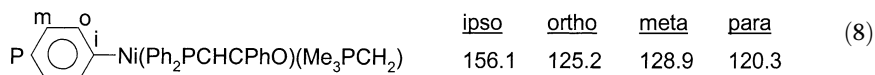
1.2.2

Spectroscopy [10–12]

Using ^{31}P NMR spectroscopy it is particularly easy to follow the reaction of the ylides **A** and **B** with the nickel(0) complex. The spectrum shows the rapid disappearance of the two ylide resonances with the simultaneous formation of two new phosphororganic moieties “ P_A ” and “ P_B ”. The reaction solution ($\text{Ni}(\text{COD})_2/\text{Ph}_3\text{PCHCHPhO}/\text{Me}_3\text{PCH}_2/\text{toluene}$) displays the new resonances in a 1:1 ratio. A well-resolved 7 Hz doublet fine structure from $^{31}\text{P}_\text{A} - ^{31}\text{P}_\text{B}$ spin–spin coupling proves that the two newly formed phosphorus groups are building blocks in a common molecular structure. The assignment is evident from the ^1H -coupled ^{31}P NMR spectrum, in which the strongly down-field shifted signal P_A of the trimethylphosphine-methylene moiety displays a characteristic multiplet splitting due to coupling with 9 equivalent H atoms from the trimethyl-P group and 2 equivalent H atoms from the P-methylene group. The slightly shifted resonance P_B of the coordinated benzoyl derivative is only broadened by ^1H -coupling [Eq. (7)].

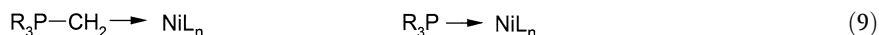
The Ni-phenyl group(Ph)

This is the other C-bound ligand. It originates from an oxidative addition of a P-phenyl moiety to nickel(0). In this way nickel binds to P and phenyl in a *cis* fashion. Accordingly, the phenyl group has a heavily deshielded ipso C atom with a two-bond *cis* coupling ${}^2J({}^{31}\text{P}^{13}\text{C})_{cis}=31\text{ Hz}$. The highfield shifts of the ortho and para C signals are indicative of a phenyl group bound to an electron-rich center (Ni). The chemical shift behavior is reminiscent of benzyl-Grignard reagents and benzyldiene phosphoranes [Eq. (8)].

**The PO Chelate Ligand (Ph₂PCHCPhO)**

The Ni–P complexation generates a four-coordinate phosphorus and the ligand may be viewed as a metallated ylide structure in a bis(ylide)nickel environment. The α carbon of the stabilized ylide remains trigonal planar after complexation, as indicated by the one-bond (${}^{13}\text{C}^1\text{H}$) coupling of 163 Hz. The double bond, which can be formulated as a phosphinoenolate structure, is strongly polarized. Owing to a partial negative charge, C- α is shifted upfield by approximately 50 ppm compared with “normal” sp^2 centers at 128 ppm. Accordingly, C- β is strongly deshielded.

The pronounced differences in the electronic structure of phosphanes R_3P and highly polar ylides R_3PCH_2 are clearly visible in valence electron photoelectron spectra (UV-PES) in that the outermost electrons of ylides (n_{C^-}) are energetically more readily available than those of corresponding phosphanes (n_P) (see Tab. 1.1). This feature is “sensed” by the nickel core electrons of related complexes [Eq. (9)]

**ESCA**

The ESCA (X-ray photoelectron spectroscopy) of related nickel complexes shows the $2p_{3/2}$ binding energy of the nickel center of $[\text{NiPh}(\text{Ph}_2\text{PCHCMeO})(\text{Ph}_3\text{PCH}_2)] = 853.4\text{ eV}$ is lower than that of $[\text{NiPh}(\text{Ph}_2\text{PCHCMeO})(\text{Ph}_3\text{P})] = 854.4\text{ eV}$ by 1 eV and thus it falls into the range of zerovalent nickel complexes! Obviously, the nickel center experiences an energetic destabilization similar to ylide C-substituents [Eq. (5)].

1.2.3

X-ray Structure Analysis [11]

The basic structure 1 is structurally related to complexes of types 2 and 3 (Tab. 1.3). A comparison is of interest because of the marked differences in activity and selectivity of ylide catalysts 1, phosphane catalysts 2, and *cis*- $[\text{Ni}(\text{PO})_2]$ bis(chelate) complexes 3. The ylide catalysts 1 are significantly more active and produce higher molecular weight products than corresponding phosphane catalysts 2. The bis(chelate) complexes 3 can be detected as polymerization-inactive decomposition products of 1 and 2, e.g. after completed oligo- or polymerization.

Tab. 1.3 Bond lengths in (PCCONi) metallocycles

Related (PO) Nickel Complexes	$d(\text{NiO})$	$(\text{CO}) [\text{\AA}]$
$[\text{NiPh}(\text{Ph}_2\text{PCHCMeO})(i\text{-Pr}_3\text{PCH}_2)]$ 1b	1.951	1.302
$[\text{NiPh}(\text{Ph}_2\text{PCHCPhO})(\text{PPh}_3)]$ 2	1.914	1.313
$[\text{Ni}(\text{Ph}_2\text{PCHCPhO})_2]$ 3	1.885	1.318

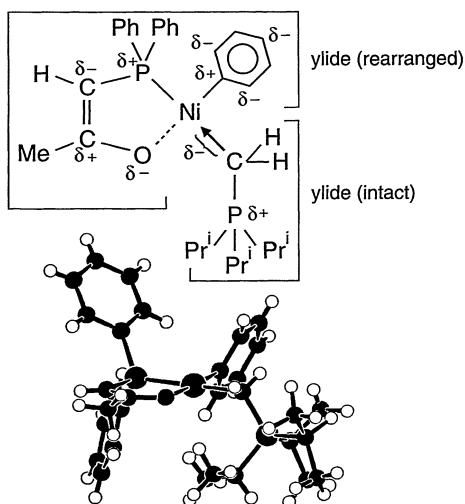


Fig. 1.2 X-ray structure and charge distribution of the bis(ylide)nickel catalyst $[\text{NiPh}(\text{Ph}_2\text{PCHCMeO})(i\text{-Pr}_3\text{PCH}_2)]$.

An X-ray structure determination of $[\text{NiPh}(\text{Ph}_2\text{PCHCMeO})(i\text{-Pr}_3\text{PCH}_2)]$ (Fig. 1.2) confirms the presence of a structurally intact C-coordinated $i\text{-Pr}_3\text{PCH}_2$ -ylide ligand in the *trans* position to the diphenylphosphino group of a $\text{Ph}_2\text{PCHCMeO}$ -PO chelate. The most striking finding is a dramatic increase in the Ni–O bond length to 1.95 Å as a consequence of a structurally intact coordinated ylide ligand (Tab. 1.3). The stepwise weakening of the Ni–O bond correlates with enhanced catalyst activity.

In summary, prominent features of ylide nickel complexes versus phosphane complexes have been identified: an electron-rich nickel center, energetically destabilized nickel-localized occupied orbitals, a significant weakening of the Ni–O bond, the phosphorus moiety being located outside the nickel coordination plane, thus opening one axial position in the nickel coordination sphere for easy monomer “landing”.

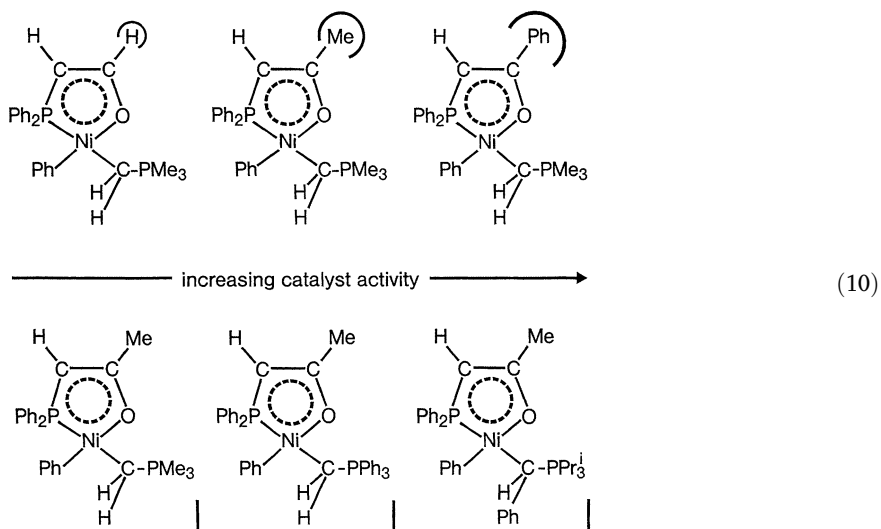
1.3

Ethylene Polymerization

1.3.1

Catalyst Activity [10, 12, 13]

Different ligand properties affect the homogeneously catalyzed oligo-/polymerization of ethylene. The nickel catalysts with structurally intact ylide ligands have considerably higher activities than comparable nickel phosphane systems. The Me_3P -nickel complex is even catalytically inactive. Frontier orbitals, as well as activity of the catalysts are influenced by variations of the intact ylide ligand. Interestingly, when the chelating acetylmethylene-triphenylphosphorane is kept unchanged, the turnover increases with decreasing first ionization potential of the structurally intact coordinating ylides [Eq. (10), bottom].



Likewise, the phosphorus-31 coordination chemical shift ($\Delta\delta\text{P reori/coord}$) of the chelate-phosphorus reflects the properties of the intact steering ligand which are transmitted by the nickel into the metallocycle. The “intact ylide”-dependent chemical shift behavior is mirrored in the activity profile of the catalyst system [12].

When, on the other hand, the intact ylide ligand Me_3PCH_2 is retained [Eq. (10), top], the turnover increases in the sequence formyl-, acetyl-, benzoyl-methylene-triphenylphosphorane, at 10 bar and approximately 100°C , to around 0.5×10^5 mole reacted ethene per mole nickel per hour. This corresponds to a catalyst activity of 1.4×10^6 g PE or 1.4 tons PE produced per mole of catalyst without using any co-catalyst or noncoordinating anions.

1.3.2

Novel Ligand Control of PE Molecular Weight [13]

GC analyses of the reaction solutions show the formation of the homologous series of ethene oligomers butene, hexene, octene, decene, etc. While the phosphane-induced Schulz-Flory distributions fall off rapidly, the ylide-derived catalysts favor formation of higher oligomers. Oligomers above C₄₀ are detectable. Both ylide ligands affect the ratio of the reaction rates propagation/termination. The quotient of the corresponding rate constants can be derived from neighboring GC peaks.

The intrinsic viscosities of the solid oligo-/polyethenes from ylide-steered nickel-catalyzed polymerizations are higher than those produced by related Ni-phosphane systems. Provided the polymer structure remains unchanged, the “Ni-ylide-steered” products consist of longer macromolecules and, accordingly, have higher molecular weights. IR data show correspondingly fewer end groups (methyl or vinyl) per 1000 C. The DSC curves of the low-melting “Ni-phosphane-steered” oligoethenes are contrasted by higher melt temperatures in ylide catalysis. GPC investigations confirm the expected higher molecular weights for the ylide-derived products.

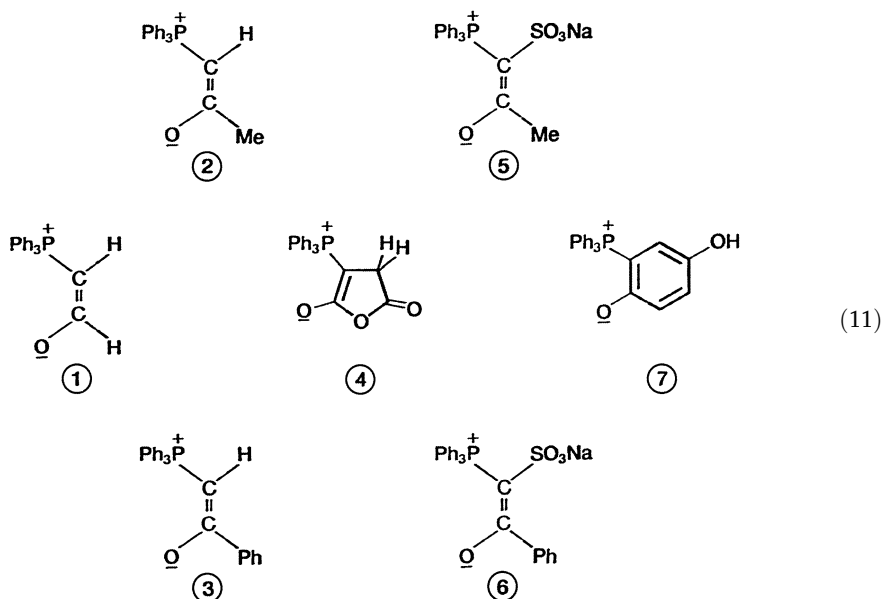
In the above-mentioned bis(ylide)nickel series [Eq. (10), top], where the intact ylide ligand Me₃PCH₂ is kept constant and the PO component is changed at the β-position from H → Me → Ph, substituting the formyl-methylenephosphorane at the β-position with a methyl group (hyperconjugation in acetyl-methylenephosphorane) affects the catalytic cycle with respect to turnover and polymer properties; the effect is even greater for substitution by a phenyl group (π-conjugation in benzoyl-methylenephosphorane). The catalyst activity increases – and so does the intrinsic viscosity of the PE formed, from approximately 0.05 to approximately 0.13 dL g⁻¹. Chain propagation as opposed to chain termination and chain transfer are favored by the ligand field modifications.

We therefore looked for other (R₃P–C=C–O) components in the (ylide A/ylide B/Ni) concept that would allow us to control the molecular weight to a greater extent.

Indeed, more marked chemical changes in the PO component dramatically altered the selectivity for the PE molecular weight and led to a *novel* ligand-steered molecular weight control. The molecular weight increases in the ligand series 1 → 2 → 3 → 4 → 5 → 6 → 7 [Eq. (11)].

A sulfonate substituent at the α-position results in high molecular weight PEs. The already mentioned β-substituent effects on the PE molecular weight can be detected here again, i.e. the sulfonated benzoyl derivative exceeds the acetyl derivative. Incorporating the α- and the β-carbon into a ring system also increases the molecular weight, with phosphane-chinone adducts being at the top of the scale.

An extreme range of high to ultra-high molecular weight PE is accessible by using an in-situ catalyst, obtainable by reacting 1 mmol of each of the three components Ni(COD)₂/Ph₃P-benzochinone/Ph₃PCH₂ in 10 ml toluene at 50 C for 2 hours. The heterogeneous reaction mixture catalyzes the polymerization of ethyl-



ene for example in cyclohexane at 10 bar and polymerization temperatures between 10 C and 150 C. The intrinsic viscosities measured in *o*-dichlorobenzene at 140 C and therefrom calculated viscosity average PE molecular weights depend strongly on the polymerization temperature.

150 C PE sample	0.89 dl/g	44 000 g/mol
130 C PE sample	1.53 dl/g	97 000 g/mol
110 C PE sample	3.60 dl/g	328 000 g/mol
90 C PE sample	5.65 dl/g	624 000 g/mol
70 C PE sample	9.12 dl/g	1 237 000 g/mol
50 C PE sample	10.01 dl/g	1 412 000 g/mol
30 C PE sample	12.62 dl/g	1 965 000 g/mol
20 C PE sample	13.27 dl/g	2 112 000 g/mol
10 C PE sample	14.19 dl/g	2 324 000 g/mol

High temperature GPC studies show that the 20 C PE sample is monomodal and has a narrow molecular weight distribution. The polydispersity M_w/M_n of 2.4 indicates a single site insertion mechanism. With increasing polymerization temperature the molecular weight distribution broadens.

Further chemical fine tuning has been achieved by means of additional ligands with ylide-type bond systems from the iso-electronic series of highly polar P-ylides, P-imines and P-oxides. Examples for HDPEs (high density polyethylenes) are given in Tab. 1.4.

No oligomers are detectable in solution. Some of the very high molecular weight polymers show long chain branching. This observation may indicate that part of the molecular weight build-up may originate from reincorporation of vinyl-

Tab. 1.4 Polyethylene properties obtained with [Ni/Ph₃P–BC/R₃PX] catalysts

<i>In situ</i> catalyst: Ni(COD) ₂ Ph ₃ P–BC	T_p [°C]	η [dL g ⁻¹]	ρ [g cm ⁻³]
Ph ₃ PO	65–85	9.60	0.968
(PhO) ₃ PO	60–100	5.85	0.960
Me ₃ PO	75–80	4.29	0.968
(Me ₂ N) ₃ PO	90	2.43	0.972
(MeO) ₃ PO	90–100	1.40	0.969

Abbreviations used: *in situ* catalyst: 2 mmol of each component preformed for 1 h at 50 °C; Ni(COD)₂: bis(cyclooctadiene)nickel(0); Ph₃P–BC: 1/1 adduct of triphenylphosphane and *p*-benzochinone; Me: methyl; Ph: phenyl; T_p : polymerization temperature; T_m : melt temperature (DSC); η : intrinsic viscosity, measured in tetraline at 140 °C; ρ : PE density. Polymerization conditions: *in situ* catalyst in 50 mL toluene, solvent: cyclohexane, ethylene pressure: 100 bar.

terminated high molecular weight PE chains. High density polyethylenes are usually unbranched and characterized by a density $\rho = 0.96\text{--}0.97\text{ g cm}^{-3}$.

An outstanding property is the systems tolerance towards solvents of different polarity with respect to maintaining catalyst activity, while at the same time creating an additional tool to control molecular weight. Increasing polarity results in reduced molecular weight. Thus, nickel catalysts with ylide ligands have for the first time opened access to all molecular weight ranges up to 10^6 g mol^{-1} and above; from ethene oligomers to polymers – from liquid α -olefins to soft and hard waxes and further up to HDPE and even ultrahigh molecular weight polyethylene (UHMW PE) with DSC melt temperatures up to 137 °C.

1.3.3

Linear and Branched Macromolecules [14]

“Tailor-made materials” require access to linear as well as to branched macromolecular structures. FTIR spectra of the polymer and GC analysis of the oligomers in solution (if present) can be used for characterization and as a reference for structural changes.

1.3.3.1 Linear Macromolecules

The selectivity of the bis(ylide)nickel catalysts frequently favors the formation of linear macromolecules with unsaturated end groups. In this case the FTIR spectrum of a PE film of defined thickness shows almost exclusively methyl and vinyl end groups. Their presence in equal quantities proves linearity. An example for the catalytically controlled formation of linear, unbranched macromolecules is given in Eq. (12).

[NiPh(Ph ₂ PCHCMeO)(Pr ₃ PCHPh)]	12	vinyl per 1000 C	(12)
	0.2	vinylidene per 1000 C	
	0.4	trans-vinylene per 1000 C	
	12	methyl per 1000 C	

A mean degree of polymerization of 42 and a molecular weight M_n of approximately 1200 g mol⁻¹ can be estimated from the quantitative end group determination in the given example.

Gas chromatographic analysis identifies the oligomers in the reaction solution as an homologous series of linear α -olefins in the range C₄ to C₄₀.

1.3.3.2 Short Chain-Branched Macromolecules

A conventional approach to the controlled formation of short-chain branches is ethene copolymerization with co-monomers such as propene, butene(1), 4-methylpentene(1), hexene(1) or octene(1). In the ethene/propene copolymerization example given below an increased number of methyl groups compared with vinyl end groups is consistent with a propene incorporation of approximately 6 mol% [Eq. (13)], the observed lower DSC melt temperatures and lower densities are typical for medium density (MDPE) and linear low density polyethylene (LLDPE).

Ni(0)/Ph ₃ PC(SO ₃ Na)CPhO/Ph ₃ PCHCHCHPh	6	vinyl per 1000 C	(13)
	0.2	vinylidene per 1000 C	
	0.4	trans-vinylene per 1000 C	
	35	methyl per 1000 C	

Ylide nickel-catalyzed ethylene polymerizations can also produce branched macromolecules from ethylene alone (that is *without* adding a co-monomer) due to ligand effects, which induce a nonlinear specificity. This “self-branching” can be achieved with special ylide ligand combinations and adequate reaction conditions, which allow the insertion of olefins other than ethylene into Ni–H and/or Ni–C bonds. Low ethylene pressure and high catalyst concentrations favor self-branching. With the catalyst shown in Eq. (14), almost equal quantities of vinylidene, *trans*-vinylene and vinyl double bonds are formed. The excess methyl content versus the total number of double bonds per 1000 carbon atoms, and the appearance of significant amounts of vinylidene groups, indicate a branched structure.

Ni(0)/Ph ₃ PC(CMeO) ₂ /Ph ₃ PCH ₂	9	vinyl per 1000 C	(14)
	9	vinylidene per 1000 C	
	9	trans-vinylene per 1000 C	
	57	methyl per 1000 C	

The appearance of *vinylidene* double bonds may be interpreted by successive chain growth, chain termination by β -H elimination with formation of α -olefin,